Voidage Wave Instability in a Vibrated Liquid-Fluidized Bed

Eldin Wee Chuan Lim and Chi-Hwa Wang

Department of Chemical and Biomolecular Engineering, National University of Singapore, 4 Engineering Drive 4, Singapore, 117576

Introduction

Liquid fluidized beds in narrow tubes are well known to be susceptible to instabilities under certain operating conditions. One such instability is the appearance of one-dimensional voidage waves consisting of alternating regions of high and low particle concentrations along the bed. Several experimental studies on such phenomenon have been reported in the literature. Duru et al.[1] investigated experimentally this type of instability by measuring the shape of these voidage waves and relating them to solid phase viscosity and pressure functions of a continuum two-phase model. Duru and Guazzelli[2] observed the formation of bubbles in the same type of system resulting from the destabilization of such voidage wave structures and compared their experimental observations with previous analytical and numerical studies. Nicolas et al.[3] also investigated the nature of such instabilities in liquid fluidized beds and suggested that the behavior of an unstable bed exhibiting voidage waves is determined by the external perturbations imposed and that the resulting instabilities are convective in nature.

Numerical Method

In the present study, the convective nature of voidage wave instabilities was investigated computationally using the Discrete Element Method (DEM) coupled with Computational Fluid Dynamics (CFD). The geometry of the fluidization system simulated consisted of a two-dimensional narrow channel of width 2 cm containing 2500 glass beads as the solids phase and water as the interstitial fluid. Each glass bead had a diameter of 1.0 mm and density 2500 kg m^{-3}. The superficial velocities of the liquid used were 0.018 m s^{-1} and 0.03 m s^{-1}. The base of the fluidization system was allowed to undergo simple harmonic motion when desired in order to facilitate the study of the effects of external perturbations on the stability of the bed. The amplitude and frequency applied when a vibrating base was simulated were 1.5 times the diameter of a glass bead (1.5 mm) and 2 Hz respectively.

Following Cundall and Strack[4], the equations in DEM governing the translational and rotational motions of individual solid particles are:

$$m_i \frac{dv_i}{dt} = \sum_{j=1}^{N} \left(f_{c,ij} + f_{d,ij} \right) + m_i g + f_{f,i} \tag{1}$$

$$I_i \frac{d\omega_i}{dt} = \sum_{j=1}^{N} T_{ij} \tag{2}$$

where m_i and v_i are the mass and velocity of particle i, N is the number of particles in contact with this particle, $f_{c,ij}$ and $f_{d,ij}$ are the contact and viscous contact damping forces respectively, $f_{f,i}$ is the fluid drag force due to an interstitial fluid, I_i is the moment of inertia of particle i, ω_i is its angular velocity and T_{ij} is the torque arising from contact forces which will cause the particle to rotate. The normal ($f_{cn,ij}$, $f_{dn,ij}$) and tangential ($f_{ct,ij}$, $f_{dt,ij}$) components of the contact and damping forces are calculated according to a linear force-displacement model:

$$f_{cn,ij} = -\left(\kappa_{n,i} \delta_{n,ij} \right) n_i \tag{3}$$

$$f_{ct,ij} = -\left(\kappa_{t,i} \delta_{t,ij} \right) t_i \tag{4}$$

$$f_{dn,ij} = -\eta_{n,i}\left(v_r \cdot n_i\right)n_i \tag{5}$$

$$f_{dt,ij} = -\eta_{t,i}\left[\left(v_r \cdot t_i\right)t_i + \left(\omega_i \times R_i - \omega_j \times R_j\right)\right] \tag{6}$$

where $\kappa_{n,i}$, $\delta_{n,ij}$, n_i, $\eta_{n,i}$ and $\kappa_{t,i}$, $\delta_{t,ij}$, t_i, $\eta_{t,i}$ are the spring constants, displacements between particles, unit vectors and viscous contact damping coefficients in the normal and tangential directions respectively, v_r is the relative velocity between particles and R_i and R_j are the radii of particles i and j respectively. If $\left|f_{ct,ij}\right| > \left|f_{cn,ij}\right|\tan\phi + c$ then 'slippage' between the two contacting surfaces is simulated by a Coulomb-type friction law, $\left|f_{ct,ij}\right| = \left|f_{cn,ij}\right|\tan\phi + c$ where $\tan\phi$ is analogous to the coefficient of friction and c is a measure of cohesion between the two contacting surfaces.

The fluid drag force model due to Di Felice[5] which is applicable over a wide range of particle Reynolds numbers was used for evaluating the fluid drag force. The equations in this model include:

$$f_{f,i} = f_{f0,i}\varepsilon_i^{-\chi} \tag{7}$$

$$f_{f0,i} = 0.5c_{d0,i}\rho_f\pi R_i^2\left|u_i - v_i\right|\left(u_i - v_i\right) \tag{8}$$

$$\chi = 3.7 - 0.65\exp\left[-\frac{\left(1.5 - \log_{10}Re_{p,i}\right)^2}{2}\right] \tag{9}$$

$$c_{d0,i} = \left(0.63 + \frac{4.8}{Re_{p,i}^{0.5}}\right)^2 \tag{10}$$

$$Re_{p,i} = \frac{2\rho_f R_i\left|u_i - v_i\right|}{\mu_f} \tag{11}$$

where $f_{f0,i}$ is the fluid drag force on particle i in the absence of other particles, χ is an empirical parameter, ε_i is the local average porosity in the vicinity of particle i, $c_{d0,i}$ is the drag coefficient, $Re_{p,i}$ is the Reynolds number based on particle diameter, ρ_f is the fluid density, μ_f is the fluid viscosity and u_i is the fluid velocity.

The motion of the continuum gas phase is governed by the Navier-Stokes equations with interphase interactions taken into account as an additional source term in the momentum equation:

$$\frac{\partial\varepsilon}{\partial t} + \nabla\cdot\left(\varepsilon u\right) = 0 \tag{12}$$

$$\frac{\partial\left(\rho_f\varepsilon u\right)}{\partial t} + \nabla\cdot\left(\rho_f\varepsilon uu\right) = -\varepsilon\nabla P + \nabla\cdot\left(\mu_f\varepsilon\nabla u\right) + \rho_f\varepsilon g - F \tag{13}$$

where u is the velocity vector, ε is the local average porosity, P is the fluid pressure and F is the source term due to fluid-particle interaction.

Experimental Method
The fluidized bed apparatus in this study consisted of four major components: a vertical cylindrical column, rotameters, centrifugal pump and liquid tank. The experimental setup is shown schematically in Figure 1a. The cylindrical column was a glass tube of 2 cm diameter and 1 m height. The bed was fluidized by water at ambient condition. During experiments, the bed was

clamped in position to maintain it vertical and straight. A centrifugal pump was used to circulate the water from the liquid tank through rotameters to the bed in a closed loop.
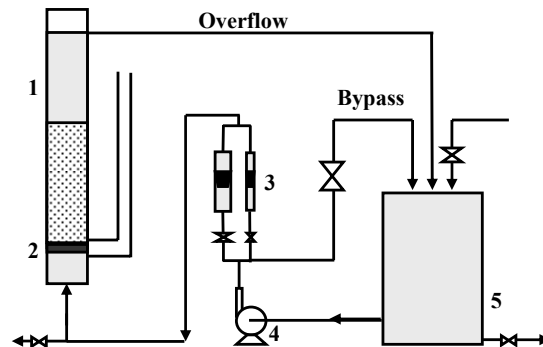
Figure 1a Schematic diagram of the liquid fluidized bed setup: 1. Vertical cylindrical bed; 2. Piston-like distributor; 3. Rotameters; 4. Centrifugal pump; 5. Liquid tank.

The bed suspension was supported by a specially designed piston, which consisted of a 2 mm thick sintered stainless steel plate with 50 μm orifice holes. These small orifice holes ensured a large pressure drop and uniform distribution of flow.[6] The piston could be set to oscillate vertically at a given frequency and amplitude driven by a stepper motor. Such a piston-distributor setup would allow examination of the response of the bed towards external perturbations. The amplitude of the piston was carefully chosen as 1.5 times the particle diameter to avoid close packing in the near distributor region.[1]

The ratio of bed to particle diameters should be greater than 10, but not exceed 25 to ensure smooth propagation of one-dimensional voidage-wave structures along the bed.[1,6] In the present study, the granular material used was glass beads of density 2500 kg/m^3 and diameter 1 mm ($u_{mf} \approx 0.01$ m s^{-1}). The corresponding bed to particle diameter ratio was then 20. The column was filled with glass beads up to a height of 12 cm and fluidized by water at flow velocities in the range 0.018 – 0.030 m s^{-1}. External harmonic perturbations were introduced into the bed by oscillating the piston-distributor with an amplitude of 1.5 mm and frequencies in the range 1 – 2 Hz. Typically, four regimes could be observed during experiments: packed, worming, planar wave and turbulent regimes. The scope of the present study was limited to the planar wave regime.

Solid concentrations were determined using a light scattering method at various bed levels. The basic principle of this technique is that under column backlighting conditions, the light intensity transmitted through the bed suspension varies strongly as a function of solid concentration. Here, a stabilized He-Ne laser (25 mW) was used as the light source and a low-energy photodiode (Newport, USA) was used to detect the transmitted intensity signals.

The velocity field data of the bed was obtained using a PowerView PIV (Particle Image Velocimetry) system from TSI Company (Figure 1b). The column was placed inside a square glass tube of dimensions 2.7 cm × 2.7 cm to facilitate more accurate measurements using the PIV system. New-Wave Nd:Yag lasers operating at ~15 mJ/pulse were introduced from the side wall of the square tube to illuminate particles near the central region of the column. Images of the illuminated particles were acquired by a TSI PowerView camera (2K × 2K resolution) at an angle perpendicular to the laser sheet. The PIV sampling frequency did not match the vibrating frequency of the moving piston. To overcome this problem, the PIV system was operated under external trigger mode with a sampling frequency of 5 Hz. The motions of particles in one full oscillation cycle of the base could then be extracted from the images captured.
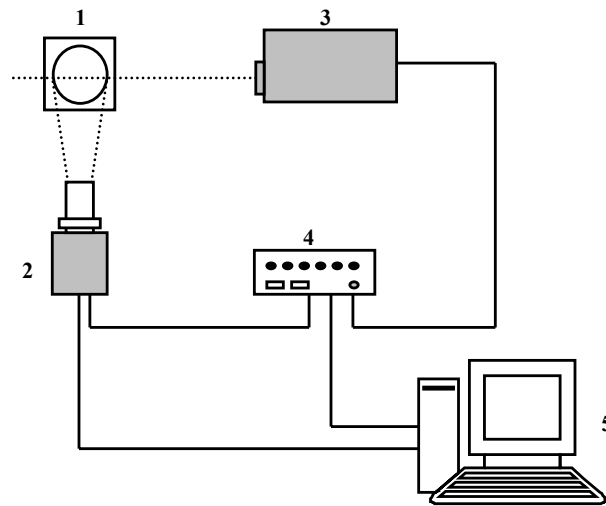
Figure 1b Schematic diagram of velocity data acquisition system (PIV system): 1. Test section; 2. PIV camera; 3. New Wave Nd:Yag laser; 4. TSI synchronizer; 5. Computer for data post-processing.

Results and Discussion

Figure 2 shows 4 consecutive snapshots of the fluidized bed system obtained from the simulation. The time interval between each snapshot is 0.05 s and the dimensions are 16 cm (height) by 2 cm (width). Alternating bands of dense and dilute solid concentrations may be clearly discerned from the figure. There are approximately two dense and two dilute phases present in the system under the present set of operating conditions. The coherent motion of these phases of the voidage wave up along the fluidized bed may also be observed. As such, the present simulation has been successful in reproducing the main qualitative feature of the phenomenon associated with voidage wave instability in a liquid fluidization system. It may also be stated that in the absence of a vibrating base, the fluidized bed was observed to expand slightly upon introduction of liquid with a superficial velocity and remain homogeneously fluidized with minimal tendency to develop such voidage wave instability. This implied that the system was intrinsically stable in the absence of external perturbations while any internal noises were not sufficiently significant to cause instability. This was true for both liquid superficial velocities of 0.018 m s^{-1} and 0.030 m s^{-1} investigated in the initial

phase of the present study. At the lower liquid superficial velocity of 0.018 m s^{-1} and in the presence of a vibrating base, a small amount of voidage waves could be observed in the system. These formed at the vibrating base but were propagated only a short distance up the bed. As the fluidized bed at this low superficial velocity was only expanded slightly and close to a packed condition, the likely reason for attenuation of the voidage waves could be the high effective solid viscosity. In contrast, when the liquid superficial velocity applied was 0.030 m s^{-1} such that the bed was expanded to a larger extent, voidage instabilities in the form of waves of high and low solid concentrations could be observed traveling up the expanded bed as shown in Figure 2. These clearly show the unstable nature of the system towards external perturbations and the convective characteristic of the resulting instability. In the following section, quantitative analyses of this phenomenon would be provided.
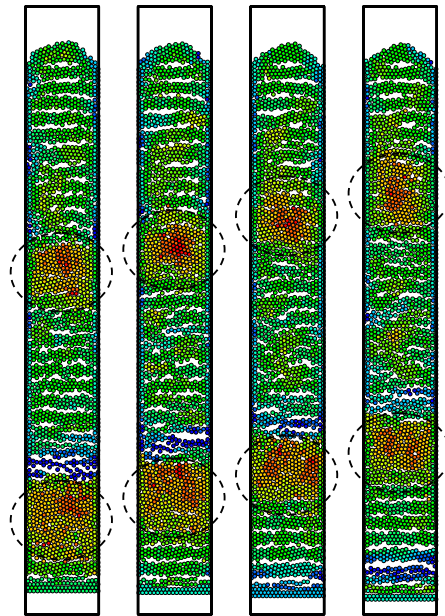
Figure 2 Voidage waves in a liquid fluidized bed operating at the following conditions: Liquid superficial velocity at inlet of 0.03 m s^{-1}, vibrating amplitude and frequency of base of 1.5 mm and 2 Hz respectively. Time interval between each frame shown is 0.05 s. Dimensions of the system are 16 cm (height) by 2 cm (width).

Figure 3a shows the instantaneous velocity vectors of particles in a section of the system about 5 cm above the vibrating base obtained from the CFD-DEM simulation. Correspondingly, Figure 3b shows the velocity vectors obtained from the experimental setup using the PIV system. Each frame of the figure shows approximately half a channel and has dimensions 1.5 cm (height) by 1.0 cm (width) with one wall of the channel on the left and the centerline on the right. The frames were captured at 0.2 s intervals. The figure illustrates the unique behavior of solid particles in a liquid fluidization system in the presence of voidage waves. Here, adopting an Eulerian point of view, it may be seen that particles switch periodically between generally upward and downward motions. These correspond to the passage of dense and dilute phases of the voidage wave through the particles respectively. In other words,

when a dense phase of the wave propagates through a section of the bed, particles in that section were observed to be moving in the upward direction and vice versa. For the present case studied, the frequency and amplitude of the vibrating base were 2 Hz and 1.5 mm respectively. Both Figures 3a and 3b show that the characteristic frequency of the periodic motion of the solid particles is also about 2 Hz. The characteristic length scale of the size of a dense (or dilute) region of the voidage wave is that of the Eulerian cell used, that is, about 1.0 – 1.5 cm.

Figure 4a shows the ensemble averaged profile of the vertical component of solid velocities at 5 cm above the vibrating base with respect to time. This shows quantitatively the oscillatory behavior of particle motion over two cycles. Figure 4b shows the corresponding power spectrum obtained by fast Fourier Transform (FFT) of the original instantaneous velocity signals. It may be observed that the characteristic frequency of the oscillatory solid velocity matches that of the vibrating base as mentioned earlier. Figure 4c shows the waveform for solid velocity obtained by ensemble averaging over 120 sets of PIV experimental data. Each set of solid velocity data was taken over a duration of 3 s. The number of experimental data sets used in the ensemble averaging has been verified to be sufficiently large to ensure statistical invariance of the resulting waveform. To the knowledge of the authors, this is the first report of such a statistical representation of the solid velocity in a liquid fluidized bed exhibiting voidage wave instability. It may be

(a)　　　　　　　　　　　　　　　**(b)**
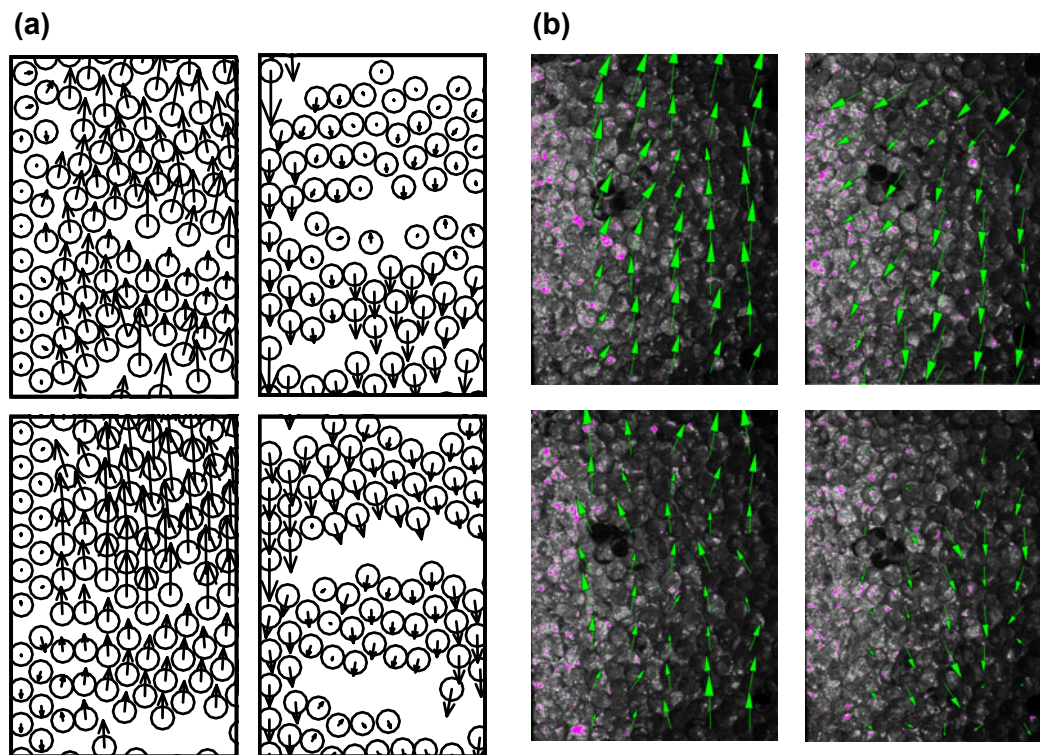
Figure 3 Instantaneous particle velocity vector field in a 1.5 cm (height) by 1.0 cm (width) section at 5 cm above the vibrating base obtained from (a) CFD-DEM simulations (b) Experiments. Snapshots are shown at 0.2 s intervals.
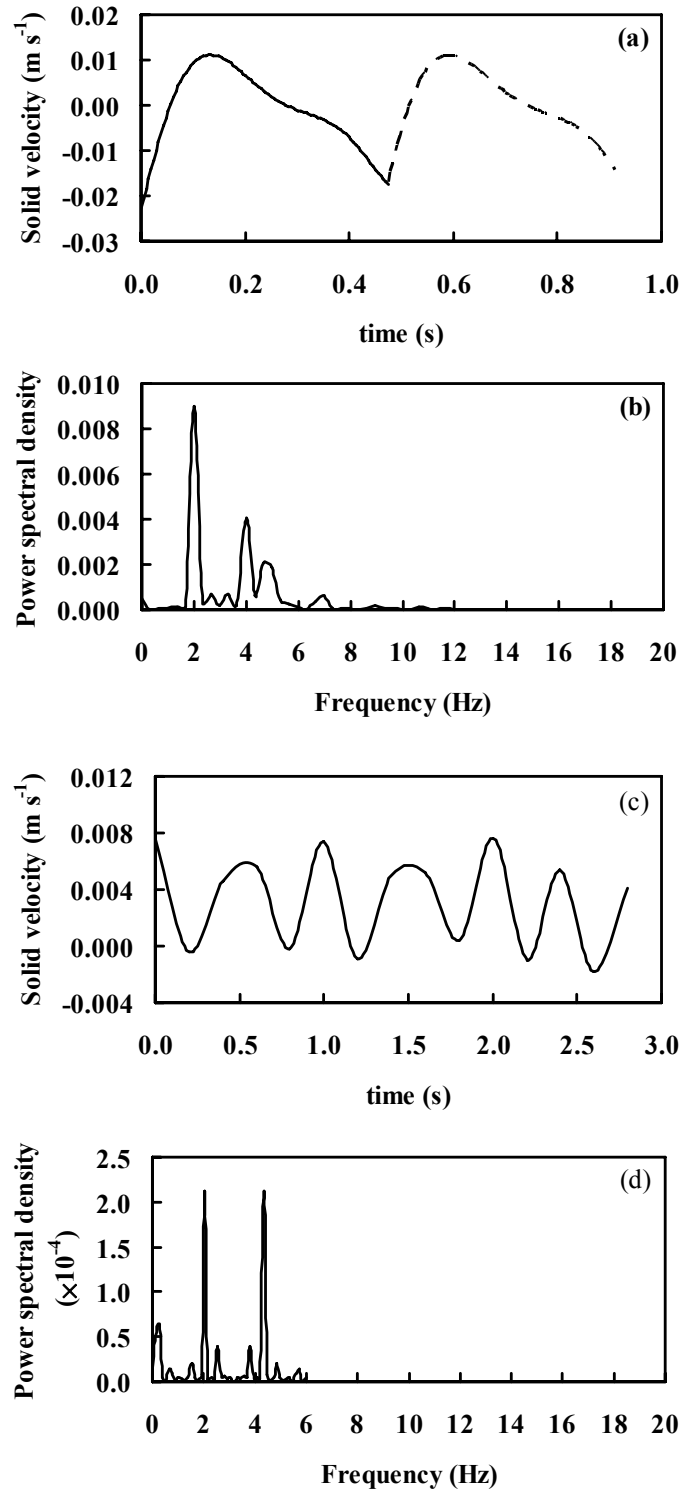
Figure 4 Ensemble averaged variation of spatially averaged vertical component of solid velocities at 5 cm above the vibrating base with respect to time obtained from (a) CFD-DEM simulations and (c) Experiments. Corresponding power spectral density of the time varying solid velocities obtained from (b) CFD-DEM simulations and (d) Experiments.

noted that ensemble averaging was only performed using six sets of solid velocity data from the CFD-DEM simulations, each over one wave cycle or corresponding to about 0.5 s, due to high computational requirements. The second cycle of the waveform shown in dashed line in Figure 4a is a replica of the first cycle and was added to aid in visualizing the periodic nature of the solid velocity. Nevertheless, the power spectral for both simulation and experimental data (Figures 4b, d) show that the dominant oscillating frequency of solid velocity is equal to that of the driving frequency of the external perturbation imposed.

Figures 5a, b show the ensemble averaged solid fraction profile at the same position (5 cm above the vibrating base) with respect to time and the corresponding power spectrum of the solid fraction signal respectively obtained from CFD-DEM simulations. As with the case for solid velocity data described above, Figure 5c shows the corresponding data obtained from the experiments conducted and ensemble averaged over 120 waveforms for solid volume fraction. Similarly, Figure 5d shows quantitatively that the characteristic frequency of the voidage wave is also equal to that of solid velocity. In addition, there may be higher or lower harmonics in the vicinity of this characteristic frequency (in the range 1 – 5 Hz) (Figure 5b).
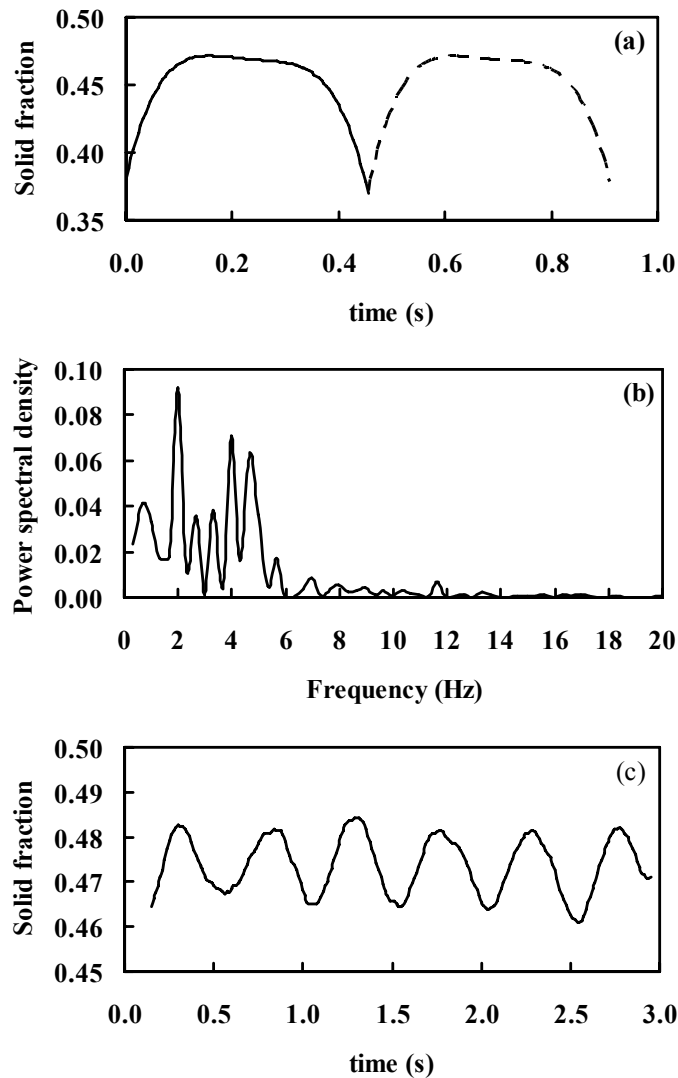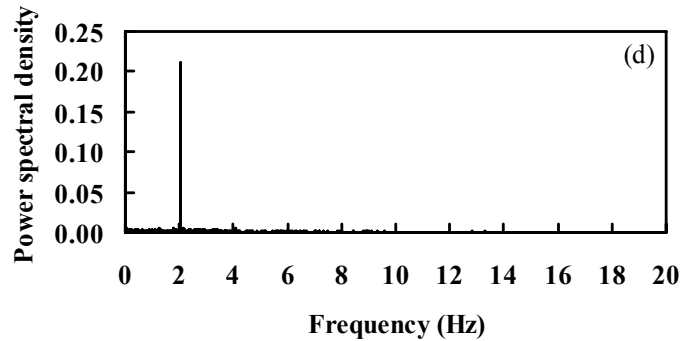
Figure 5 Ensemble averaged variation of spatially averaged solid fraction at 5 cm above the vibrating base with respect to time obtained from (a) CFD-DEM simulations and (c) Experiments. Corresponding power spectral density of the time varying solid fraction obtained from (b) CFD-DEM simulations and (d) Experiments.

Conclusions

The nature of one-dimensional voidage waves in a liquid fluidized bed subjected to external perturbations and exhibiting instabilities has been investigated both experimentally and numerically. Voidage waves consisting of alternating regions of high and low solid concentrations were observed to form and travel in a coherent manner along the fluidized bed. Solid particles were seen to move upwards when a dense phase of the wave passed through their positions and settle downwards otherwise. The voidage waves formed as a result of instability in such liquid fluidized bed systems are traveling waves with dense and dilute phases being convected along the bed. However, the motion of individual particles was observed to be highly restricted to a small region or cell over short time scales. A diffusive type of behavior was observed where particles drifted gradually away from their initial positions within the bed. This type of motion was adequately described by a simple dispersion model used in the present study.

Literature Cited

1. Duru, P., M. Nicolas, J. Hinch, E. Guazzelli. Constitutive laws in liquid-fluidized beds. Journal of Fluid Mechanics, *452*, 371–404. 2002.
2. Duru, P. and E. Guazzelli. Experimental investigation on the secondary instability of liquid-fluidized beds and the formation of bubbles. Journal of Fluid Mechanics, *470*, 359–382. 2002.
3. Nicolas, M., J.-M. Chomaz, D. Vallet, E. Guazzelli, E. Experimental investigations on the nature of the first wavy instability in liquid fluidized beds. Physics of Fluids, *8*, 1987–1989. 1996.
4. Cundall, P. A. and O. D. L. Strack. A discrete numerical model for granular assemblies. Geotechnique, *29*, 47–65. 1979.
5. Di Felice, R. The voidage function for fluid-particle interaction systems. Int. Journal Multiphase Flow, *20*, 153–159. 1994.
6. Ham, J. M., S. Thomas, E. Guazzelli, G. M. Homsy, M.-C. Anselmet. An experimental study of the instability of liquid-fluidized beds. International Journal of Multiphase Flow, *16*, 171–185. 1990.